Stanford Exploration Project, Report 92, November 12, 1997, pages 191–208

Azimuthal behavior of P-waves in horizontal transverse isotropy

Héctor Urdaneta[1]

keywords: *modeling, amplitudes, diffraction, anisotropy, density*

ABSTRACT

The behavior of P-wave reflection varies with azimuth for rocks whose material properties vary with azimuth. I study the effects of horizontal transverse isotropy in P-wave reflection patterns on a simple homogeneous model, a finely fractured shale overlying an isotropic chalk with varied amounts of fracturing. I have produced 2-D reflectivity maps that clearly illustrate the azimuthal behavior of P-waves as the aspect ratio, volume density and filling material of the cracks are varied.

INTRODUCTION

Modeling plane-wave reflection and transmission coefficients at a plane interface between two homogeneous half spaces is a fundamental problem in wave propagation with many geophysical applications. Zoeppritz's research (1919) was among the first theoretical work to study the solution for this problem in the case of two isotropic media. Ostrander (1984) was one of the first to use these results assuming isotropic media for doing amplitude versus offset analysis (AVO). In order to apply AVO analysis on azimuthally-anisotropic targets such as fracture reservoirs, anisotropy must be accounted for in modeling the reflection coefficients. In my opinion, while in some cases anisotropic AVO behavior for a given azimuth can be explained by an equivalent isotropic model, azimuthal variations are a better indicator of reflectivity changes.

It is important to study reflection amplitudes for anisotropic materials as a first step in modeling azimuthal anisotropic AVO signatures. To date only numerical modeling is available to fully model reflection amplitudes. Recently, Rüeger (1995) obtained approximate expressiones for P-wave reflection coefficients in transversely isotropic media; however, he assumes weak anisotropy, small discontinuities in elastic properties across boundaries, and the bulk of his analyses are confined to symmetry planes. Unfortunately, while symmetry planes are an understandable and tractable case, they are also a misleading special case. Anisotropic phenomena must be studied

[1]**email:** hector@sep.stanford.edu

as a 3-D problem. While the precise behavior of such phenomena can be described mathematically, the analytical expressions are usually too complex to allow any comprehension, including the case of transverse isotropy, which is the next level up in complexity after isotropy.

In the quest to obtain an approximate expression of reflection amplitudes, valid for any propagation direction, any degree of anisotropy, and any degree of discontinuity in the elastic parameters across the boundaries, I look at the effects of horizontal transverse isotropy in P-wave reflection patterns on a simple anisotropic model, a finely fractured shale overlying an Austin Chalk with varied amounts of fracturing. I investigate whether it is feasible to determine the parameters, content, and orientation of fractures from azimuthal variations in P-wave reflectivity measurements and conclude that we get indications when plotting 2-D views even for pre-critical angles.

To check the validity of these modeling results with real applications, we must assume a medium where anisotropy has a much higher order effect than heterogeneity in wave propagation. We also must assume planar interfaces and that we are working in the far field approximation, in order to satisfy the hypothesis that plane waves expand the solution space of anisotropic wave propagation.

The first section of this paper reviews the theory on plane-wave propagation in a homogeneous medium. The second section follows along the lines of Dellinger's (1991) work on plane wave propagation for a horizontally transverse isotropy media. The third section focuses on plane wave propagation across horizontal interfaces for homogeneous half spaces following the work of Nichols (1991) on his two-way phase-shift modeling scheme. In the final section, I compute reflectivity maps with a modified version of Nichols's phase-shift modeling scheme.

WAVE EQUATION AND PLANE WAVE SOLUTIONS

When considering plane waves propagating in a homogeneous anisotropic medium, it is convenient to use the Christoffel equation. This equation is simply the elastodynamic wave equation Fourier transformed over space and time. It specifies the propagation velocity and particle-motion (also called *polarization*) direction for each plane-wave component in the Fourier domain. The Christoffel equation takes the form of a simple eigenvalue-eigenvector problem, as follows:

$$\begin{aligned} \mathbf{D}\mathbf{C}\mathbf{D}^T\vec{\mathbf{v}} &= \rho\left(\frac{\omega}{k}\right)^2\vec{\mathbf{v}} \qquad (1) \\ \mathbf{D} &= \frac{1}{k}\begin{pmatrix} k_x & 0 & 0 & 0 & k_z & k_y \\ 0 & k_y & 0 & k_z & 0 & k_x \\ 0 & 0 & k_z & k_y & k_x & 0 \end{pmatrix} \end{aligned}$$

where ρ and the 6×6 symmetric matrix $\mathbf{C}$ define the homogeneous medium, ρ is the density, and $\mathbf{C}$ (in compressed notation) gives the elastic constants. The derivative matrix $\mathbf{D}$ defines the direction of plane-wave propagation. The leading $\frac{1}{k}$ term normalizes the wavenumber vector ($k = |\vec{\mathbf{k}}| = \sqrt{k_x^2 + k_y^2 + k_z^2}$). The terms ω and $\vec{\mathbf{v}}$ define the resulting wave modes; $\vec{\mathbf{v}}$ is the particle-motion direction, and ω is the associated phase velocity.

Solving the eigensystem in equation (1) is straightforward. For any wavenumber vector $\vec{\mathbf{k}}$, the symmetry of the matrix $\mathbf{DCD}^T$ ensures that the underlying eigenvalue-eigenvector problem is well-behaved: we can always find three distinct modes associated with three orthogonal directions of particle motion. This eigensystem has solutions only when its determinant vanishes:

$$\det |\mathbf{DCD}^T - \rho \left(\frac{\omega}{k}\right)^2 \mathbf{I}| = 0$$

For a general anisotropic medium, this equation requires the solution of a third-order polynomial in $\rho \left(\frac{\omega}{k}\right)^2$, where we can identify the term ω/k as the velocity V_ω of the plane wave with direction $\vec{\mathbf{k}}/k$, which results in

$$\det |\mathbf{DCD}^T - \rho V_\omega^2 \mathbf{I}| = 0 \tag{2}$$

The three roots, which correspond to the eigenvalues of equation (1) are the velocities of the three fundamental plane waves. The eigenvectors of equation (1) are, respectively, the three directions of particle motion. In general, none of these fundamental waves will be purely longitudinal or purely transverse.

TRANSVERSE ISOTROPY

The simplest physically realizable anisotropic system is hexagonal symmetry anisotropy, known as *transverse isotropy* (TI). Hexagonal symmetry has an axis of cylindrical symmetry, which implies that the properties of the medium in a given direction depend only on the angle between that direction and the symmetry axis direction. The symmetry direction is usually a result of some dominant global directed influence, such as gravity, regional stresses or parallel cracks. If gravity causes it, then the symmetry axis lies vertically, and the medium has transverse isotropy with a vertical axis of symmetry (VTI). If the direction of symmetry results from horizontal regional stresses or vertically parallel cracks, the symmetry axis lies horizontally, and the medium has transverse isotropy with a horizontal axis of symmetry (HTI).

Mathematics of transverse isotropy with a horizontal axis of symmetry

The elastic modulus matrix of an HTI medium with a symmetry axis along the x direction (which I will denote as HTI_x) has the following form (in compressed notation):

$$C_{\alpha\beta} = \begin{pmatrix} c_{11} & c_{13} & c_{13} & 0 & 0 & 0 \\ c_{13} & c_{33} & c_{33}-2c_{44} & 0 & 0 & 0 \\ c_{13} & c_{33}-2c_{44} & c_{33} & 0 & 0 & 0 \\ 0 & 0 & 0 & c_{44} & 0 & 0 \\ 0 & 0 & 0 & 0 & c_{55} & 0 \\ 0 & 0 & 0 & 0 & 0 & c_{55} \end{pmatrix} \tag{3}$$

This representation can easily be obtained by a $\frac{\pi}{2}$ rotation of the VTI's elastic matrix along the y axis. Incorporating this expression into equation (1) and identifying ω/k as the velocity V_ω of the plane wave with propagation direction (k_x, k_y, k_z) gives us

$$\begin{pmatrix} c_{11}k_x^2 + c_{55}(k_y^2+k_z^2) & (c_{13}+c_{55})k_xk_y & (c_{13}+c_{55})k_xk_z \\ (c_{13}+c_{55})k_xk_y & c_{55}k_x^2 + c_{33}k_y^2 + c_{44}k_z^2 & (c_{33}-c_{44})k_yk_z \\ (c_{13}+c_{55})k_xk_z & (c_{33}-c_{44})k_yk_z & c_{55}k_x^2 + c_{44}k_y^2 + c_{33}k_z^2 \end{pmatrix} \begin{pmatrix} v_x \\ v_y \\ v_z \end{pmatrix} = \rho V_\omega^2 \begin{pmatrix} v_x \\ v_y \\ v_z \end{pmatrix} \tag{4}$$

From here on, to simplify notation, I use the variables $\delta_{33} = c_{33} - c_{55}$, $\delta_{11} = c_{11} - c_{55}$, and $\chi = c_{13} + c_{55}$, introduced by Dellinger (1991). Thus we rewrite equation (4) as

$$\begin{pmatrix} c_{11}k_x^2 + c_{55}(k_y^2+k_z^2) & \chi k_xk_y & \chi k_xk_z \\ \chi k_xk_y & c_{55}k_x^2 + c_{33}k_y^2 + c_{44}k_z^2 & (c_{33}-c_{44})k_yk_z \\ \chi k_xk_z & (c_{33}-c_{44})k_yk_z & c_{55}k_x^2 + c_{44}k_y^2 + c_{33}k_z^2 \end{pmatrix} \begin{pmatrix} v_x \\ v_y \\ v_z \end{pmatrix} = \rho V_\omega^2 \begin{pmatrix} v_x \\ v_y \\ v_z \end{pmatrix} \tag{5}$$

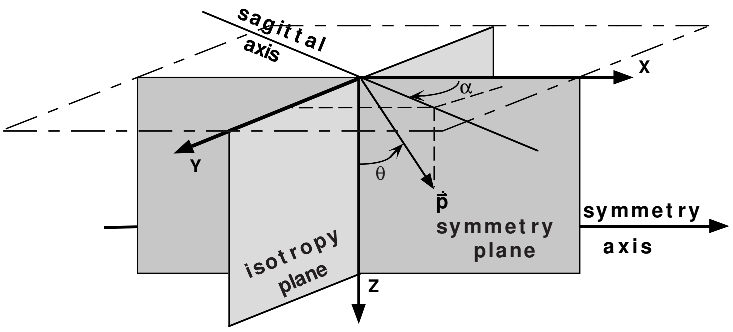

Figure 1: Definition of propagation angles. The azimuthal angle α is measured with respect to the symmetry axis, and the incidence angle θ with respect to the vertical axis. hector1-HTIprop [NR]

Plane wave modes

Considering nondispersive media, for the propagation direction $k_x = k\sqrt{\sin^2\theta\cos^2\alpha}$, $k_y = k\sqrt{\sin^2\theta\sin^2\alpha}$, and $k_z = k\sqrt{\cos^2\theta}$, where the angles θ and α are measured from the vertical axis and the medium's symmetry axis, respectively, as shown in Figure 1, equation (5) produces the following three plane wave modes (results obtained with the symbolic calculation software package Mathematica):

$$\rho V_\omega^2 = c_{44}\,(1-k_x^2) + c_{55}k_x^2 \quad \text{and} \quad \begin{pmatrix} v_x \\ v_y \\ v_z \end{pmatrix} = \gamma \begin{pmatrix} 0 \\ -k_z \\ k_y \end{pmatrix} \tag{6}$$

where γ is an arbitrary constant, usually taken as a normalizing factor.

This is a pure shear mode, since its direction of particle motion $(0, -k_z, k_y)$ is always perpendicular to the direction of propagation (k_x, k_y, k_z). This propagation mode is called an *SH mode.*

The other two solutions are expressed as follows:

$$\begin{aligned} \rho V_\omega^2 &= \frac{1}{2}\Big\{(c_{33}+c_{55})(1-k_x^2) + (c_{11}+c_{55})k_x^2 \\ &\pm \sqrt{(\delta_{11}k_x^2 - \delta_{33}(1-k_x^2))^2 + 4\chi k_x^2(1-k_x^2)}\Big\} \qquad \text{and} \\ \begin{pmatrix} v_x \\ v_y \\ v_z \end{pmatrix} &= \gamma \begin{pmatrix} \delta_{11}k_x^2 - \delta_{33}(1-k_x^2) \pm \sqrt{(\delta_{11}k_x^2 - \delta_{33}(1-k_x^2))^2 + 4\chi k_x^2(1-k_x^2)} \\ 2\chi k_x k_y \\ 2\chi k_x k_z \end{pmatrix} \end{aligned} \tag{7}$$

The sign of "±" selects one of the two remaining modes. The "+" sign selects the "fast" wave solution, while the "−" sign selects the "slow" wave solution. For all angles of direction θ and α, the fast solution is always greater than the slow solution. In the case of isotropy, the fast solution corresponds to the P-wave solution, the slow to the SV-wave. For transverse isotropy and for anisotropy in general, the fast wave-mode may be neither a pure P-wave nor an approximate P-wave, just as the slow wave-mode may be neither a pure SV-wave nor an approximate SV-wave. For this reason and to avoid bias, it is better to call these two solutions the *fast* and the *slow* wave solutions, instead of using the conventional notation, qP and qS.

It is important to notice that any plane wave propagating in the $y-z$ plane, will have a constant-value velocity function. This plane is referred to as the *isotropy plane* (Figure 1).

Even though it may not be obvious from equations (6) and (7), the three propagation modes, fast, slow, and SH, are perpendicular to each other as expected.

REFLECTION AND TRANSMISSION COEFFICIENTS

To propagate plane waves across a horizontal interface between two transversely isotropic homogeneous media, we must proceed somewhat different than previously. Because we do not know what the vertical wavenumber component will be across a horizontal interface (Snell's law only guarantees the continuity of the horizontal slownesses), we must solve the eigensystem in equation (1) in terms of p_z (which gives simpler expressions than solving in terms of k_z) for the upper and lower media, and impose the necessary boundary conditions at the interface. Rearranging equation (1) and expressing it in terms of slownesses, we obtain

$$\begin{aligned}(\mathbf{PCP}^T &- \rho\mathbf{I})\,\omega^2\vec{\mathbf{v}} = 0 \\ \mathbf{P} &= \begin{pmatrix} p_x & 0 & 0 & 0 & p_z & p_y \\ 0 & p_y & 0 & p_z & 0 & p_x \\ 0 & 0 & p_z & p_y & p_x & 0 \end{pmatrix}\end{aligned} \tag{8}$$

where $\mathbf{I}$ is the 3×3 identity matrix.

Computing this system's eigenvalues requires the solution of a sixth- order polynomial in p_x, p_y, and p_z. The solution expresses the vertical slowness p_z as a sixth-order polynomial of a pair of horizontal slownesses p_x and p_y. If the system has monoclinic symmetry or higher, as is the case of transverse isotropy, we only need to solve a cubic polynomial in p_z^2.

Each of the six eigenvalues p_z^λ corresponds to a particle-motion direction $\vec{\mathbf{v}}_\lambda$. Wave-types are separated into three up-going and three down-going by computing the z-component of their Poynting vector. Its sign gives the sense of direction of the vertical energy flow.

Plane wave solutions

For a plane wave with horizontal slownesses p_x and p_y and frequency ω, the total displacement vector $\vec{\mathbf{u}}$ at some point in space $\vec{\mathbf{x}}$ is given by

$$\vec{\mathbf{u}} = \sum_{\lambda=1}^{6} S_\lambda \vec{\mathbf{v}}_\lambda e^{i\omega(t - \vec{\mathbf{x}}\cdot\vec{\mathbf{p}}^\lambda)} \tag{9}$$

where $\vec{\mathbf{p}}^\lambda = (p_x, p_y, p_z^\lambda)^T$. The summation is over the six wave-types in the medium, which have slowness vectors $\vec{\mathbf{p}}^\lambda$, particle-motion direction $\vec{\mathbf{v}}_\lambda$, and amplitudes S_λ.

The strains in the medium are given by $e_{kl} = \frac{1}{2}(u_{k,l} + u_{l,k})$, the stresses by $\tau_{ij} = C_{ijkl}e_{kl}$.

Boundary conditions at a horizontal interface

At a horizontal interface, we assume a displacement-stress vector whose variables are continuous across the interface $(\vec{\mathbf{u}}, \boldsymbol{\tau_N})$, where $\vec{\mathbf{u}} = (u_x, u_y, u_z)^T$ is the velocity, and $\boldsymbol{\tau_N} = -1/(i\omega)\,(\tau_{xz}, \tau_{yz}, \tau_{zz})^T$ represents the vertical component of the stress tensor. This vector can be divided into

$$\begin{pmatrix} \vec{\mathbf{u}} \\ \boldsymbol{\tau_N} \end{pmatrix} = F \cdot \vec{\mathbf{w}} \tag{10}$$

where the elements of F are

$$F_{ij} = \begin{pmatrix} v_x^1 & v_x^2 & v_x^3 & v_x^4 & v_x^5 & v_x^6 \\ v_y^1 & v_y^2 & v_y^3 & v_y^4 & v_y^5 & v_y^6 \\ v_z^1 & v_z^2 & v_z^3 & v_z^4 & v_z^5 & v_z^6 \\ \tau_{xz}^1 & \tau_{xz}^2 & \tau_{xz}^3 & \tau_{xz}^4 & \tau_{xz}^5 & \tau_{xz}^6 \\ \tau_{yz}^1 & \tau_{yz}^2 & \tau_{yz}^3 & \tau_{yz}^4 & \tau_{yz}^5 & \tau_{yz}^6 \\ \tau_{zz}^1 & \tau_{zz}^2 & \tau_{zz}^3 & \tau_{zz}^4 & \tau_{zz}^5 & \tau_{zz}^6 \end{pmatrix} \tag{11}$$

and the elements of the vector $\vec{\mathbf{w}}$ are a function of the wave amplitudes, as follows:

$$w_j(z) = S_j e^{i\omega(t - \vec{\mathbf{x}}\cdot\vec{\mathbf{p}}^j)} \tag{12}$$

To calculate the amplitude partitioning at an interface between two layers we equate the displacement-stress vector across the interface, thus:

$$F^{top} \cdot \vec{\mathbf{w}}^{top} = F^{bottom} \cdot \vec{\mathbf{w}}^{bottom} \tag{13}$$

Translating the coordinate frame so that the interface is at $z = 0$, the exponential terms in w are the same in both layers, and we can write equation (13) as

$$F^{top} \cdot \vec{\mathbf{S}}^{top} = F^{bottom} \cdot \vec{\mathbf{S}}^{bottom} \tag{14}$$

giving a general relation between the up-going and down-going wave systems in the two media. If we partition $\vec{\mathbf{S}}$ so that $\vec{\mathbf{S}}_D = (S_1, S_2, S_3)$ is a vector of the amplitudes of down-going waves and $\vec{\mathbf{S}}_U = (S_4, S_5, S_6)$ of up-going waves, we can write the block-matrix equation as

$$\begin{pmatrix} F_{11}^{top} & F_{12}^{top} \\ F_{21}^{top} & E_{22}^{top} \end{pmatrix} \begin{pmatrix} \vec{\mathbf{S}}_D^{top} \\ \vec{\mathbf{S}}_U^{top} \end{pmatrix} = \begin{pmatrix} F_{11}^{bottom} & F_{12}^{bottom} \\ F_{21}^{bottom} & F_{22}^{bottom} \end{pmatrix} \begin{pmatrix} \vec{\mathbf{S}}_D^{bottom} \\ \vec{\mathbf{S}}_U^{bottom} \end{pmatrix} \tag{15}$$

In order to calculate the up-going reflected wavefield and the down-going transmitted wavefield for a downward propagating wavefield incident on the boundary from above, we need to solve the system

$$\begin{pmatrix} F_{11}^{top} & F_{12}^{top} \\ F_{21}^{top} & E_{22}^{top} \end{pmatrix} \begin{pmatrix} \vec{\mathbf{S}}_D^{top} \\ \vec{\mathbf{S}}_U^{top} \end{pmatrix} = \begin{pmatrix} F_{11}^{bottom} & F_{12}^{bottom} \\ F_{21}^{bottom} & F_{22}^{bottom} \end{pmatrix} \begin{pmatrix} \vec{\mathbf{S}}_D^{bottom} \\ \vec{\mathbf{0}} \end{pmatrix} \tag{16}$$

After some manipulation, we obtain (Nichols, 1991)

$$\begin{aligned} \vec{\mathbf{S}}_U^{top} &= R_D \cdot \vec{\mathbf{S}}_D^{top} \\ \vec{\mathbf{S}}_D^{bottom} &= T_D \cdot \vec{\mathbf{S}}_D^{top} \end{aligned} \tag{17}$$

where

$$\begin{aligned} R_D &= (F_{21}^{bottom}(F_{11}^{bottom})^{-1}F_{12}^{top} - F_{22}^{top})^{-1}(F_{21}^{top} - F_{21}^{bottom}(F_{11}^{bottom})^{-1}F_{11}^{top}) \\ T_D &= (F_{11}^{bottom} - F_{12}^{top}(F_{22}^{top})^{-1}F_{21}^{bottom})^{-1}(F_{11}^{top} - F_{11}^{top}(F_{22}^{top})^{-1}F_{21}^{top}) \end{aligned} \tag{18}$$

The 3×3 matrices R_D and T_D convert the vector of down-going wave amplitudes in layer 1 into a vector of up-going reflected wave amplitudes in layer 1 and a vector of down-going transmitted amplitudes in layer 2. The next section studies the PP wave reflection amplitudes given by the first column, first row element in matrix R_D.

MODELING REFLECTIONS

In this section, I use the results obtained from equation (18) to model P-wave reflection amplitudes numerically, from a homogeneous material representing a shale overlying another homogeneous material representing an isotropic chalk matrix with a set of vertical fractures with constant azimuth. The purpose of the modeling is to study the azimuthal behavior of P-wave[2] reflection amplitudes as a function of fracture parameters.

The model is depicted in Figure 2. It is the same model used by Karrenbach et al. (1992). This work differs from theirs in that I directly model reflection amplitudes and compute 2-D raster plots that better show how different fracture parameters are related to the azimuthal behavior of reflection amplitudes. From these raster plots, we also obtain insight into how to derive an approximate expression for the reflection amplitudes. The two-layer model is composed of finely layered shales situated on top of a fractured chalk layer. The stiffness constants of these materials are given in Appendix A. The unfractured material stiffnesses are taken from data published by Wright (1987) and White (1982).

The study done on this model illustrates how different amounts of fracturing produce different azimuthal variations of the reflectivity surfaces. The isotropic chalk model is fractured using Schoenberg and Muir's (1989) group-theoretic approach (S&M), and the fracture parameters are varied using Hudson's model (Hudson, 1981). The model is built using Nichols's anisotropic model building library (Nichols, 1988), as shown in the example in Appendix B.

[2]This section uses notation loosely by calling the fast wave modes *P waves*, but just in the sense that they are primary waves, not that their polarization aligns with the direction of propagation. This terminology works fine for transverse isotropy where the fast wave modes are always faster than the other two modes. For a general anisotropic case we may not be able to call specific modes *fast* or *slow,* since their velocity surfaces may cross.

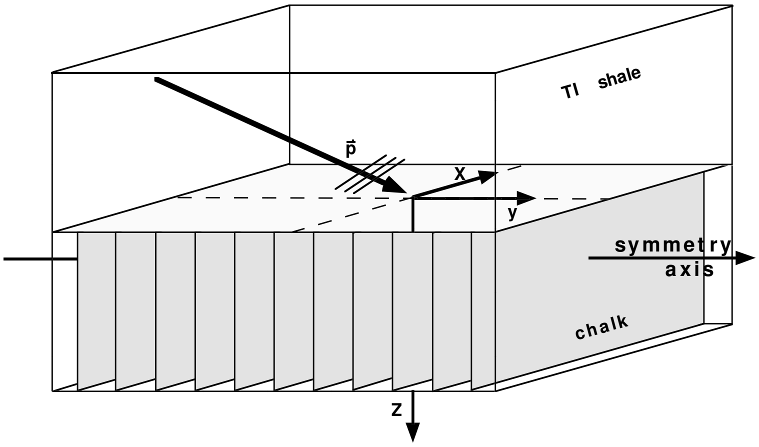

Figure 2: A homogeneous block model. The overburden is a finely layered shale, and the underlying medium is an isotropic chalk matrix with a set of vertical fractures running parallel to the x axis. hector1-model [NR]

Adding fractures

The S&M group-theoretic formalism is used to fracture the matrix rock. Fractures are treated as very thin compliant layers, which are added to the matrix rock by summing their group representations. Also, rocks are "uncracked" by subtracting their group representations.

I also use Hudson's first-order model in crack density to build penny-shaped cracks that are added to the matrix rock using S&M's group-theoretic formalism (Nichols, 1989). Both Hudson's and S&M's formulations are valid under conditions of small volume density of cracks, small crack aspect ratio, and in the long-wavelength limit.

In the first part of next section I use the S&M group theoretic formalism to add dry, wet, and air-filled cracks to the isotropic chalk. Adding dry cracks is done in the same way as for water- and air-filled cracks. I compute the fracture compliance matrix of the filling material, add it to the group representation of the matrix rock, and invert for the elastic constants of the resulting equivalent fractured medium. In the case of dry cracks, it happens that the filling material of the fracture is equal to the background material.

Since the group elements of any anisotropic system form an Abelian group, we know that the resulting elastic moduli is a stable physical "rock." Yet we must be aware of the limitations of the S&M formalism: we can only add fractures as a small excess percentage of the matrix rock, since the elastic moduli of the fracture are much smaller than a typical nonzero modulus of the background material, that is,

$$\text{rock} + \% * \text{fracture} \rightarrow \text{fracture rock}$$

In the second part of next section, I use Hudson's model of fracturing to vary the aspect ratio and the volume density of cracks. I have modeled three different types of cracks. Model A describes cracks with large aspect ratio and medium volume density, with a fluid as the crack filling material. Model B maintains the filling material but represents the other extreme, a small aspect ratio and large volume density of cracks. Model C is the chalk matrix, with a medium aspect ratio and a small volume density of cracks.

The numerical results for the PP reflection amplitudes are computed in a 70×70 grid mesh as a function of horizontal slownesses. The grid's minimum and maximum x and y slowness values are defined from the critical angle of the isotropic chalk.

Fracture direction is considered constant for all models along the x axis (see Figure 2); thus the symmetry axis of the equivalent transversely isotropic medium lies along the y axis (HTI_y).

Amplitude reflection modeling results

Figures 3 and 4 show the azimuthal behavior of the reflection amplitudes as we change the fracture contents using S&M theory. The top-left plot shows the reflection amplitudes when the underlying chalk has not been fractured. As expected from our isotropy experience, we can see that the contour lines show a circular pattern (the 70×70 grid on which the reflection amplitudes are computed produces the roughness of the contour lines). We will use this top-left plot as our comparison guide to see how the different crack fillings (and later, for the Hudson model, the cracks' shape and density) produce azimuthal behaviors away from the isotropic case. The dashed lines are constant amplitude contours. The grey color scale shows reflection amplitudes, black indicating the absence of reflections.

The top-right and bottom-left plots in Figure 3 model the reflection amplitudes for the case in which 1% excess compliance of dry cracks and air-filled cracks, respectively, have been added to the isotropic chalk. There are no visible changes from the "no cracks" plot. We use the eye as a discriminator of changes that are worth studying, that is, changes that could be detected in a surface seismic experiment.

When the cracks are filled with water (Figure 3, bottom-right plot), the changes in the reflection amplitude as a function of azimuth become evident. The impedance change between the two layers decreases along the y direction. Thus we see within the plotting window that almost all the energy is transmitted for waves propagating in the near y direction. The critical angle recedes along the y axis.

When we look Figure 4, the results look more interesting. In this figure, the experimental setup is the same as in Figure 3, but the excess compliance of the fracture crack material is changed to 10%.

Once again, dry cracks have not produced any visible azimuthal variations of the reflection amplitudes. Thus in these cases an isotropic equivalent medium can give the same answer for a surface seismic experiment as the HTI medium. The air-filled cracks now produce an elliptical pattern for the inner contour line and elongate the critical angle contour line (the long dashed line that passes by $-p_x^{\min}, 0$ and $+p_x^{\max}, 0$)

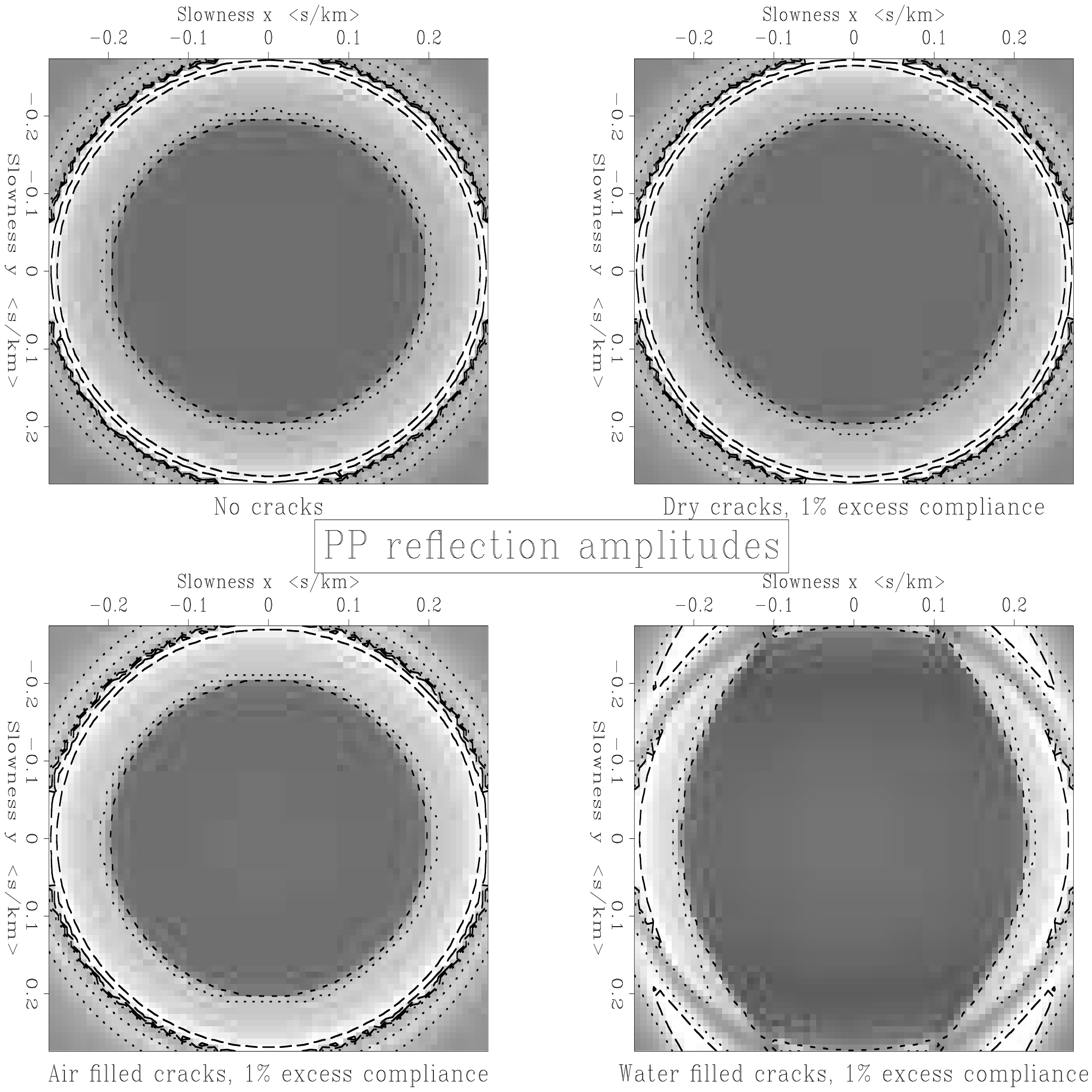

Figure 3: PP reflection amplitude comparison of low excess compliance fractures for dry, air-filled, and water-filled cracks versus the behavior of the unfractured medium. hector1-SM.1 [NR]

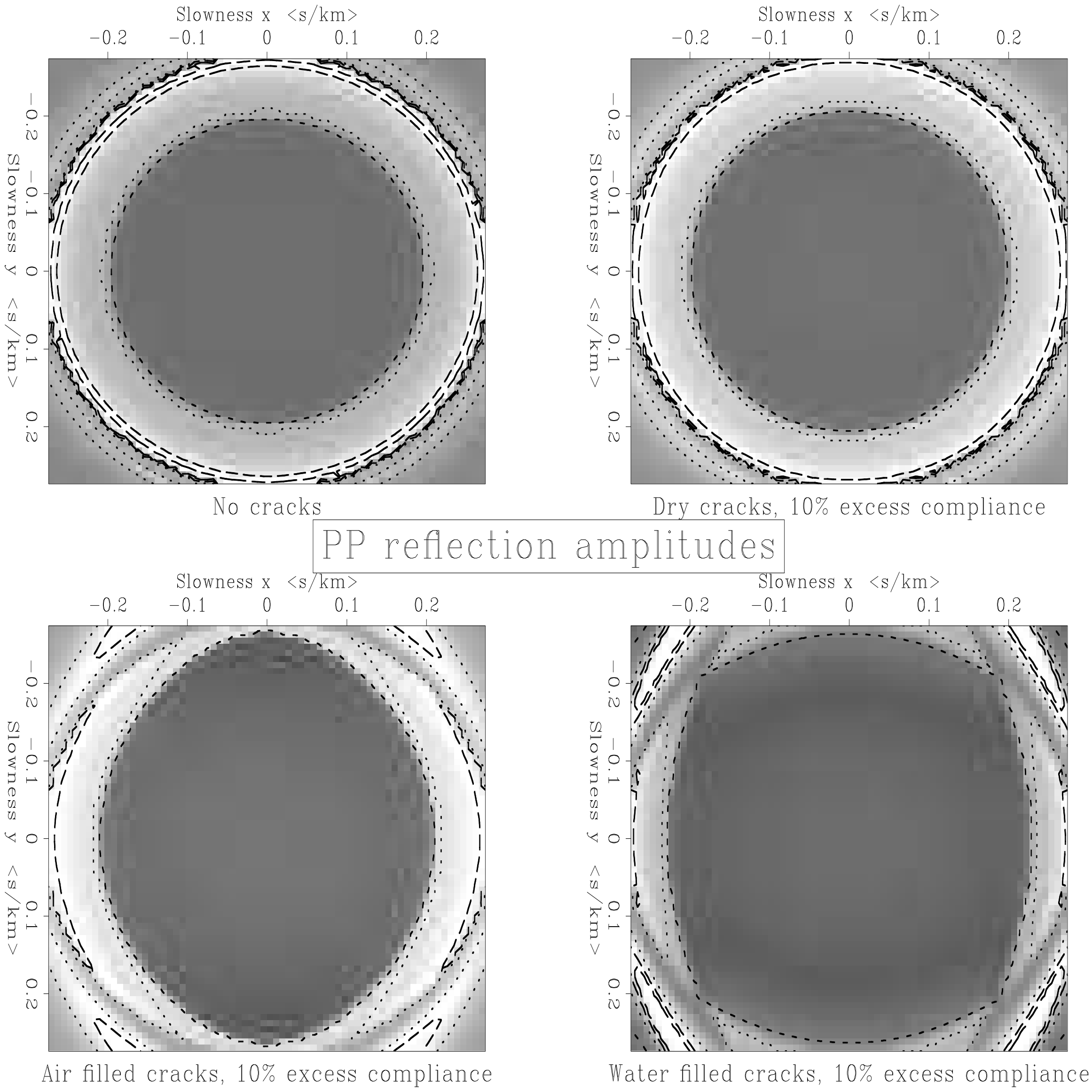

Figure 4: PP reflection amplitude comparison of high excess compliance fractures for dry, air-filled, and water-filled cracks versus the behavior of the unfractured medium. hector1-SM.10 [NR]

in the y direction.

Even more interesting is the pattern produced by the water-filled cracks. The first contour line has a double elliptic pattern (which suggests a way to obtain an approximation function for amplitude reflection). Again, the critical angle contour lines are elongated along the y direction.

Figures 5 and 6 vary the aspect ratio and volume density of the cracks. Figure 5 was produced using a low percentage of excess compliance of the filling materials, fluid and gas. None of the plots show any distinctive azimuthal behavior. The amount of fracturing is small enough that the behavior is still isotropic for P-wave reflection amplitudes.

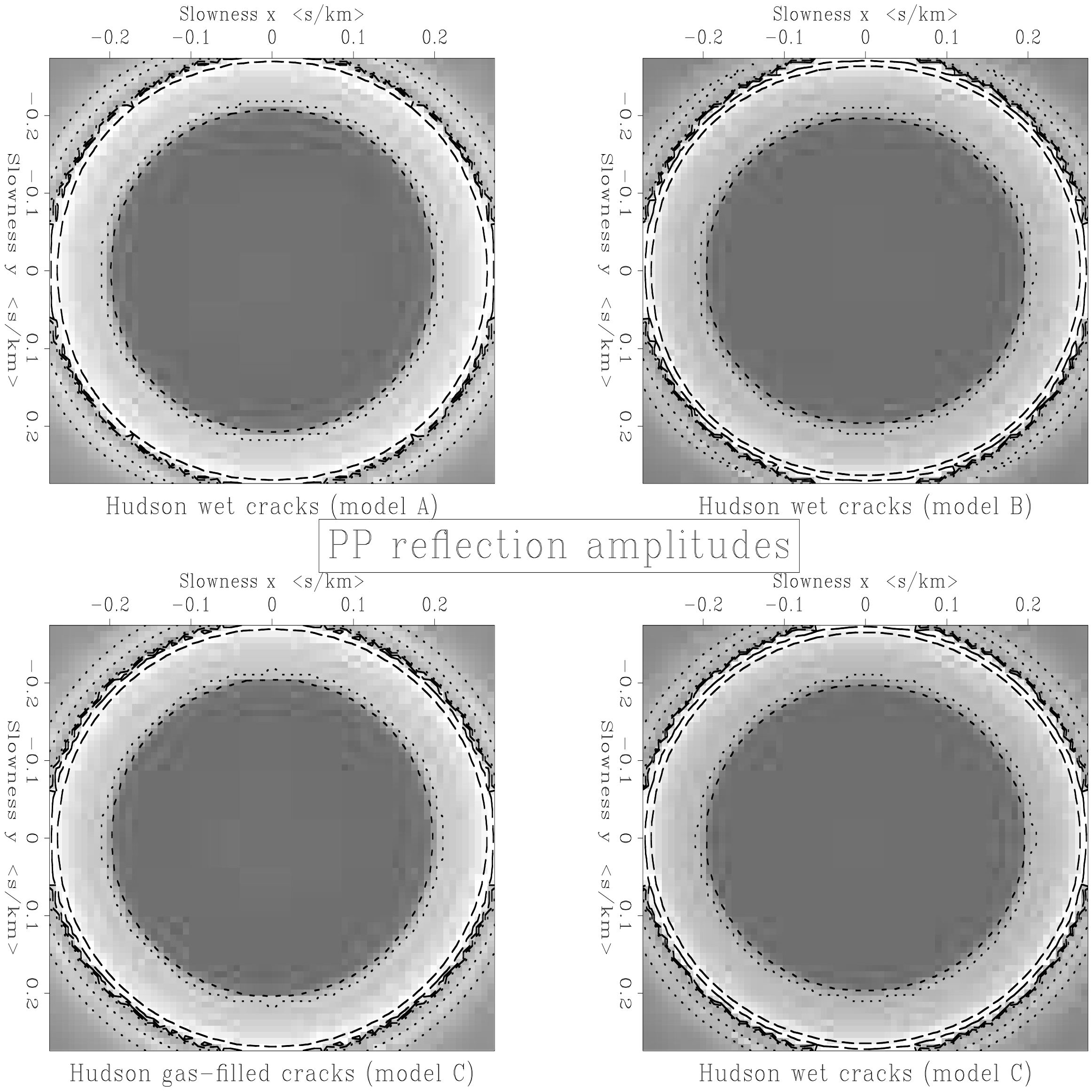

Figure 5: PP reflection amplitude comparison of models A, B, and C cracks with low excess compliances. hector1-HudABC.1 [NR]

The results in Figure 6 were obtained using a percentage of excess compliance value 10 times higher than for the preceding figure. The different results show how the behaviors differ among the different fluid-filled crack models. Models A and B show distinctive double elliptic patterns for the inner contour lines. Typically, surface seismic experiments are shot only for precritical angles; thus only the inner contour lines have an effect on 3-D AVO studies. Critical angle reflections for model A recede along the y direction, while in model B we see that the critical angle reflections do not vary with azimuth.

For gas-filled cracks in model C, we obtain the same reflection amplitude patterns as for the 10% excess compliance air-filled cracks in the S&M model (Figure 4, bottom-left plot). In model C, the fluid-filled cracks behave as in an equivalent isotropic model, not displaying any azimuthal behavior.

CONCLUSIONS

The foregoing examples show that reflection amplitudes depend on the material filling of the cracks, crack shape, and crack density. P-wave reflection magnitudes are most affected near critical angles, yet there is also significant azimuthal variation at pre-critical angles in some of the models. P-wave reflection magnitudes display different degrees of azimuthal behavior as the aspect ratio, volume density and filling material of the cracks are varied.

Generally, as we have seen, fracture direction aligns with elongation of contour lines. However, we may run into trouble for model B of cracks when trying to fit an ellipse on the P-wave pattern, as recently proposed by Lefeuvre (1994). The pattern for this model has the interesting property that azimuthal behaviors for precritical angles are only observed for out-of-axis propagation angles. All in all, the patterns obtained for the models suggest that a double elliptic approximation should be used to model P-wave reflection amplitudes. In future research, I hope to tackle the problem of obtaining an approximate theory to model TI reflection coefficients that is valid for any degree of anisotropy and of discontinuities in the elastic properties across boundaries, and valid for any angle of propagation. Such theory should reproduce the results obtained here, and explain the different behaviors.

REFERENCES

Dellinger, J., 1991, Anisotropic seismic wave propagation: SEP–**69**.

Hudson, J. A., 1981, Wave speeds and attenuation of elastic waves in material containing cracks: Geophys. J. Roy. Astr. Soc., **64**, 133–150.

Karrenbach, M., Nichols, D., and Muir, F., 1992, Modeling reflections from the Austin chalk – A practical application of azimuthal anisotropy: SEP–**75**, 251–272.

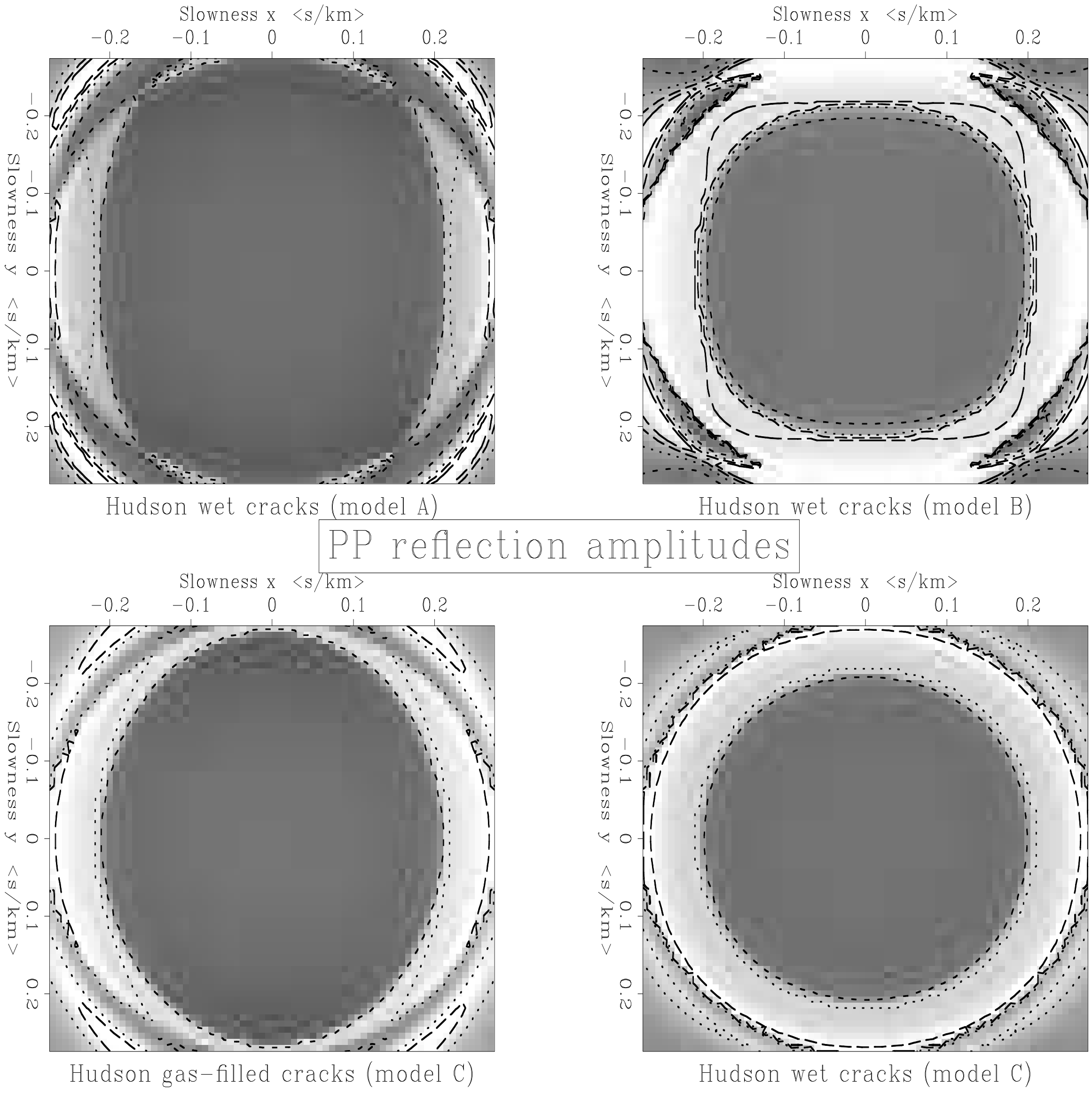

Figure 6: PP reflection amplitude comparison of model A, B, and C cracks with high excess compliances. hector1-HudABC.10 [NR]

Lefeuvre, F., 1994, Fracture related anisotropy detection and analysis: "and if the p-waves were enough": 64th Annual Internat. Mtg., Soc. Expl. Geophys., Expanded Abstracts, 942–945.

Nichols, D., 1988, Building anisotropic models: SEP–**57**, 191–206.

Nichols, D., 1989, A comparison of two models for the elastic properties of fractured rock: SEP–**60**, 261–270.

Nichols, D., 1991, A simple modeling scheme for layered anisotropic media: SEP–**70**, 337–356.

Ostrander, W. J., 1984, Plane-wave reflection coefficients for gas sands at nonnormal angles of incidence: Geophysics, **49**, no. 10, 1637–1648.

Rüeger, A., 1995, P-wave reflection coefficients for transversely isotropic media with vertical and horizontal axis of symmetry: 65th Annual Internat. Mtg., Soc. Expl. Geophys., Expanded Abstracts, 278–281.

Schoenberg, M., and Muir, F., 1989, A calculus for finely layered anisotropic media: Geophysics, **54**, no. 5, 581–589.

White, J. E., 1982, Computed waveforms in transversely isotropic media: Geophysics, **47**, no. 5, 771–783.

Wright, J., 1987, The effects of transverse isotropy on reflection amplitude versus offset: SHORT NOTE: Geophysics, **52**, no. 4, 564–567.

Zoeppritz, K., 1919, Erdbebenwellen VII B, On the reflection and penetration of seismic waves through unstable layers: Göttinger Nachrichten, **1**, 66–84.

APPENDIX A

Table of elastic constants

medium type	c11	c12	c13	c22	c23	c33	c44	c55	c66	ρ
TI shale	29.81	10.35	10.35	29.81	10.35	20.70	5.18	5.18	9.73	2.3
iso chalk	67.50	33.75	33.75	67.50	33.75	67.50	16.875	16.875	16.875	2.7
Frac chalk wet	57.32	13.40	23.57	26.80	13.40	57.32	16.875	16.875	16.875	2.7
Frac chalk air	66.34	31.44	32.60	62.88	31.44	66.34	16.875	16.875	16.875	2.7
Frac chalk dry	67.33	33.42	33.58	66.83	33.42	67.33	16.708	16.875	16.708	2.7
Model A wet	65.793	30.34	32.34	60.67	30.34	65.793	15.075	16.875	15.075	2.7
Model B wet	67.27	33.29	33.52	66.58	33.29	66.27	15.075	16.875	15.075	2.7
Model C gas	66.30	31.35	32.55	62.70	31.35	66.30	16.515	16.875	16.515	2.7
Model C wet	67.30	33.35	33.55	66.70	33.35	67.30	16.515	16.875	16.515	2.7

APPENDIX B

SEPlib's library for building anisotropic models

SEP's anisotropic model building library was written by Dave Nichols (1989), and was recently made part of the standard SEP library, thanks in part to Joe Dellinger. The library can be downloaded from SEP's ftp site. A sample shell for creating the water-filled fracture model used in the text follows.

```
503 himalaya> cat Frac.wet.csh
#!/bin/csh -f
if ( $#argv == 0 ) then
 echo  "SYNOPSIS: Frac.wet.csh excess%"
 echo  "need percentage of cracking as argument"
exit(-1)
endif
set percent = $1

echo "BOTTOM"
echo "unfractured, isotropic chalk"
create isochalk delz=1 rho=2.7 velp=5.0 vels=2.5

echo "TOP"
echo "TI shale cap-rock"
create tishale delz=1 rho=2.3  c11=29.81 c12=10.35 c13=10.35 c22=29.81 \
c21=10.35 c23=10.35 c31=10.35 c32=10.35 c33=20.7 c44=5.18 c55=5.18     \
c66=9.730

echo "FILLING"
echo "Water for filling cracks"
create water delz=1 rho=1.0  c11=2.25 c12=2.25 c13=2.25 c22=2.25       \
c21=2.25 c23=2.25 c31=2.25 c32=2.25 c33=2.25 c44=0 c55=0 c66=0

echo "Vertically cracking Chalk with $percent EXCESS filled with water"
vcrack isochalk water chalk.$percent.wet excess=$percent

# make a two layer stack (using standard SEPlib, notice the ".H" now)
Merge tishale.H chalk.$percent.wet.H axis=2 space=no > $percent.wet.mdl
```

More information about the model library can be found in Nichols's (1989) report by invoking the online documentation of the library's programs.